

# UNCOVERING EXTREMELY METAL-POOR STARS IN THE MILKY WAY'S ULTRA-FAINT DWARF SPHEROIDAL SATELLITE GALAXIES<sup>1</sup>

EVAN N. KIRBY<sup>2</sup>, JOSHUA D. SIMON<sup>3</sup>, MARLA GEHA<sup>4</sup>, PURAGRA GUHATHAKURTA<sup>2</sup>, AND ANNA FREBEL<sup>5</sup>

*Submitted to ApJL*

## ABSTRACT

We present new metallicity measurements for individual red giant branch stars in eight of the least luminous dwarf spheroidal galaxies (dSphs) in the Milky Way (MW) system. Our technique is based on medium resolution Keck/DEIMOS spectroscopy coupled with spectral synthesis. We present the first spectroscopic metallicities at  $[\text{Fe}/\text{H}] < -3.0$  of stars in a dwarf galaxy, with individual stellar metallicities as low as  $[\text{Fe}/\text{H}] = -3.3$ . Because our  $[\text{Fe}/\text{H}]$  measurements are not tied to empirical metallicity calibrators and are sensitive to arbitrarily low metallicities, we are able to probe these extremely metal-poor regimes accurately. The metallicity distribution of stars in these dSphs is similar to the MW halo at the metal-poor end. We also demonstrate that the luminosity-metallicity relation previously seen in more luminous dSph galaxies ( $M_V = -13.4$  to  $-8.8$ ) extends smoothly down to an absolute magnitude of  $M_V = -3.7$ . The discovery of extremely metal-poor stars in dSphs lends support to the  $\Lambda$ CDM galaxy assembly paradigm wherein dwarf galaxies dissolve to form the stellar halo of the MW.

*Subject headings:* galaxies: dwarf — galaxies: abundances

## 1. INTRODUCTION

In the hierarchical theory of the assembly of galaxy halos (White & Rees 1978; Searle & Zinn 1978), dwarf galaxies interact gravitationally with their hosts, shedding stars, losing gas, and eventually tidally dissolving into the diffuse halo. Recent numerical simulations and semi-analytic models (e.g., Bullock & Johnston 2005) suggest that a Milky Way-like halo can be explained entirely by disrupted satellites in the  $\Lambda$ CDM paradigm.

Clearly, dwarf galaxies must play some role in building stellar halos of large galaxies because both the Milky Way (MW) and M31 exhibit tidal streams (e.g., Ibata et al. 2001; Choi et al. 2002; Gilbert et al. 2007) and dwarf galaxies in various stages of disruption (e.g., Ibata et al. 1994; Howley et al. 2008). However, the chemical abundances of individual stars in present-day MW dSphs do not match that of the MW halo. Shetrone et al. (2001) found a lower  $[\alpha/\text{Fe}]$  for dSph red giant branch (RGB) stars than for MW halo RGB stars. The differences in chemical abundances led Tolstoy et al. (2003) to conclude that the bulk of the halo can not be composed of stars like those present in surviving dSphs.

In order to compare the bulk metallicities of stars in dSphs and the MW halo, Helmi et al. (2006, hereafter H06) obtained medium-resolution spectra of the MW dSphs Sculptor, Fornax, Sextans, and Carina. Using an empirical relation between the infrared Ca II triplet

(CaT) equivalent width (EW) and  $[\text{Fe}/\text{H}]$  (Tolstoy et al. 2001), they argue that the absence of  $[\text{Fe}/\text{H}] < -3.0$  stars in these four MW dSphs—and the presence of such stars in the MW halo—demonstrates that the halo could not have formed from ancient counterparts to the present-day dSphs. Although the metallicity distribution functions (MDFs) of the halo and the dSphs may have evolved over the age of the Universe, if dSphs once contained a population of extremely metal-poor stars, then it is difficult to understand how they could have lost *all* of those stars by the present day.

In this Letter, we reconsider the absence of metal-poor stars in MW dSphs by targeting lower luminosity galaxies and by using a more direct technique to measure  $[\text{Fe}/\text{H}]$  (based on Fe lines) than has been used before on low or moderate resolution spectra. In §2, we describe new metallicity measurements from the Simon & Geha (2007, hereafter SG07) data set of eight of the least luminous MW dSphs. Because these new measurements circumvent some problems in the CaT measurement and calibration, we are able to identify extremely metal-poor stars ( $[\text{Fe}/\text{H}] < -3.0$ ) in MW dSphs for the first time. In §3, we compare the ultra-faint dSph MDFs to the halo MDF. We also present the luminosity-metallicity relation for the full range of MW dSph luminosities. In §4, we briefly summarize our findings and discuss work on dSph chemical abundances beyond  $[\text{Fe}/\text{H}]$ .

## 2. METALLICITY MEASUREMENTS

We make use of the observations of SG07, who targeted eight of the ultra-faint dSphs discovered with SDSS: Coma Berenices, Canes Venatici I and II, Hercules, Leo IV, Leo T, and Ursa Major I and II. In summary, SG07 used DEIMOS on the Keck II telescope to obtain spectra at  $R = 6000$  over a spectral range of roughly 6500–9000 Å. This configuration is very similar to that employed by Guhathakurta et al. (2006). S/N varied widely from 5–120 Å<sup>-1</sup>.

arXiv:0807.1925v1 [astro-ph] 14 Jul 2008

<sup>1</sup> Data herein were obtained at the W. M. Keck Observatory, which is operated as a scientific partnership among the California Institute of Technology, the University of California, and NASA. The Observatory was made possible by the generous financial support of the W. M. Keck Foundation.

<sup>2</sup> University of California Observatories/Lick Observatory, Department of Astronomy & Astrophysics, University of California, Santa Cruz, CA 95064; ekirby@ucolick.org

<sup>3</sup> Department of Astronomy, California Institute of Technology, 1200 E. California Blvd., MS 105-24, Pasadena, CA 91125

<sup>4</sup> Astronomy Department, Yale University, P.O. Box 208101, New Haven, CT 06520

<sup>5</sup> McDonald Observatory, University of Texas, Austin, TX 78712

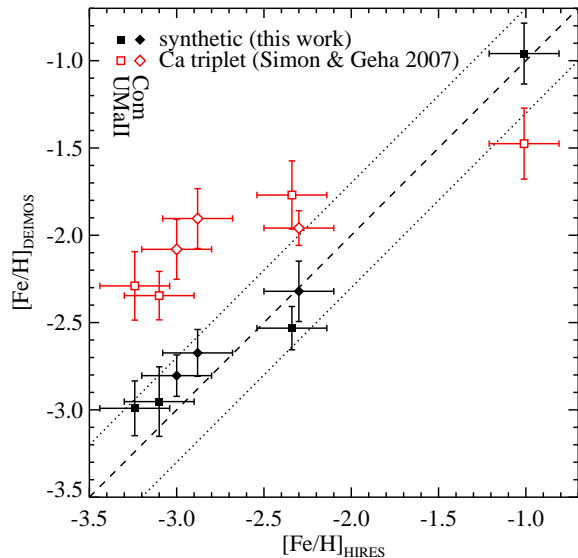


FIG. 1.— Metallicities for the RGB stars in two ultra-faint dSphs observed with both DEIMOS and HIRES. The  $x$ -axis shows the high resolution spectroscopic metallicities, and the  $y$ -axis shows two types of medium resolution spectroscopic metallicities: synthetic from this work (*black filled symbols*) and Ca triplet from Simon & Geha (2007, *red open symbols*). The synthetic metallicities are consistent with the HIRES metallicities. The dashed line is one-to-one, and the dotted lines are at  $\pm 0.3$  dex.

### 2.1. Technique

Many previous abundance studies of large samples ( $> 10$  RGB stars) of medium-resolution spectra in MW dSphs (H06, SG07, Tolstoy et al. 2004; Koch et al. 2006, 2007a,b; Bosler et al. 2007; Battaglia et al. 2006, 2008) have relied on empirical relations between the CaT and  $[\text{Fe}/\text{H}]$ . These linear relations are calibrations based on globular clusters (GCs) in the metallicity range  $-2.1 \lesssim [\text{Fe}/\text{H}] \lesssim -0.6$  (e.g., Rutledge et al. 1997) or individual stars in MW dSphs with a minimum  $[\text{Fe}/\text{H}] = -2.5$  (Battaglia et al. 2008). All of these calibrations have been shown to be accurate in their calibrated metallicity ranges. However, all of these relations are defined such that they give finite values even for a metal-free star. Therefore, they must fail at very low metallicities. Therefore, we employ a different technique to avoid the much debated issue on the metallicity at which the CaT method becomes non-linear.

Kirby, Guhathakurta, & Sneden (2008, hereafter KGS08) describe a new technique to measure metallicities from moderate resolution, far-red spectra of RGB stars. The method compares an observed spectrum to a grid of synthetic spectra at a range of effective temperatures, surface gravities, and compositions. Given a photometric estimate of temperature and gravity, the  $[\text{Fe}/\text{H}]$  of the synthetic spectrum with the best pixel-to-pixel match to the observed spectrum is the measured  $[\text{Fe}/\text{H}]$  for the star. This approach is similar to a typical high-resolution spectroscopic abundance analysis.

We exclude blue horizontal branch stars and spectra for which the S/N was too low to permit a radial velocity cross-correlation ( $\text{S}/\text{N} \lesssim 10 \text{ \AA}^{-1}$ ). We transform SDSS  $gri$  magnitudes to Johnson-Cousins  $VI$  magnitudes fol-

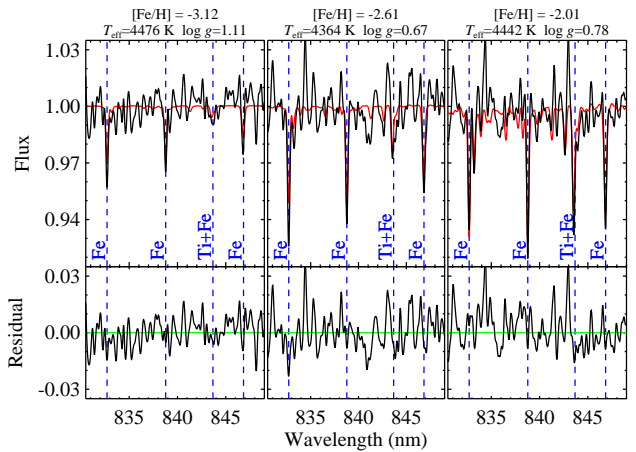


FIG. 2.— Small portions of DEIMOS spectra from three example stars at similar effective temperatures (*black*). The spectra are smoothed for clarity. The unsmoothed absorption line depths are about 2.3 times greater than shown here. Lines of Fe I and a Ti+Fe blend are labeled. The red lines in the top panels are synthetic spectra corresponding to the  $[\text{Fe}/\text{H}]$ ,  $T_{\text{eff}}$ , and  $\log g$  of the observed stars. In the bottom panels, the black lines are the differences between the observed and synthetic spectra, and the green lines are zero.

lowing Chonis & Gaskell (2008) in order to derive the temperatures ( $T_{\text{eff}}$ ) and gravities ( $\log g$ ) in the same way as KGS08. The results are unaffected by using alternative photometric transformations. In order to minimize the effect of variable  $[\alpha/\text{Fe}]$ , we mask all the spectral regions susceptible to absorption by Mg, Si, S, Ar, Ca, or Ti, which comprise 18% of the spectral range. Future work will address  $[\alpha/\text{Fe}]$  for these galaxies.

### 2.2. Assessments of the metallicities

KGS08 demonstrate their technique on Galactic GCs and show that  $[\text{Fe}/\text{H}]$  may be determined as accurately as 0.1 dex on high S/N spectra and  $\sim 0.5$  dex on spectra with S/N as low as  $10 \text{ \AA}^{-1}$ . Because the most metal-poor system that KGS08 analyze is M15 ( $[\text{Fe}/\text{H}] = -2.4$ ), we compare our metallicities to those determined from Keck/HIRES spectra of several stars in UMaII and Com that SG07 also targeted with DEIMOS. The high-resolution abundance analysis of these stars (Frebel et al., in prep.) shows that the KGS08 method accurately reproduces high-resolution abundance measurements at least down to  $[\text{Fe}/\text{H}] = -3.0$ . We emphasize that the KGS08 technique is a direct measurement of a star's iron and iron-peak absorption lines and does not make use of any calibration to obtain metallicity. Therefore, it is not restricted to any metallicity range.

Figure 1 compares both CaT (SG07) and synthetic metallicities to HIRES metallicities. The HIRES spectra favor the synthetic metallicities over the CaT metallicities. Below  $[\text{Fe}/\text{H}] < -2.5$ , the differences between the HIRES and CaT metallicities may be a result of the limitations of the CaT calibration. However, we also allow the possibility that measuring the CaT EW in DEIMOS has not been examined thoroughly enough. The DEIMOS spectra of SG07 are at a significantly higher resolution ( $R \sim 6000$ ) than the spectra from the modular spectrograph at the Las Campanas Du Pont telescope ( $R \sim 2100$ ) used for the CaT calibration adopted by SG07 (Rutledge et al. 1997). Therefore, the CaT calibration for DEIMOS spectra may ben-

TABLE 1  
ULTRA-FAINT dSPH METALLICITIES

dSph	$N^a$	$\log(L/L_\odot)^b$	$\langle[\text{Fe}/\text{H}]\rangle$	$\sigma_{[\text{Fe}/\text{H}]}$	$\log(\text{S}/\text{N})^c$
UMaII	13	$3.6 \pm 0.2$	$-2.27 \pm 0.06$	0.73	$1.6 \pm 0.4$
LeoT	19	$4.8 \pm 0.3$	$-2.02 \pm 0.05$	0.54	$1.1 \pm 0.2$
UMaI	28	$4.1 \pm 0.1$	$-2.29 \pm 0.04$	0.54	$1.5 \pm 0.3$
LeoIV	12	$3.9 \pm 0.2$	$-2.58 \pm 0.08$	0.75	$1.3 \pm 0.3$
Com	24	$3.6 \pm 0.2$	$-2.53 \pm 0.05$	0.45	$1.5 \pm 0.3$
CVnII	16	$3.9 \pm 0.2$	$-2.19 \pm 0.05$	0.58	$1.5 \pm 0.1$
CVnI	165	$5.4 \pm 0.1$	$-2.08 \pm 0.02$	0.46	$1.3 \pm 0.3$
Herc	20	$4.6 \pm 0.1$	$-2.54 \pm 0.04$	0.51	$1.6 \pm 0.4$

NOTE. — Data for individual stars (RA, Dec,  $V$ ,  $I$ ,  $\text{EW}_{\text{CaT}}$ , and  $[\text{Fe}/\text{H}]_{\text{synth}}$ ) are available on request from the first author.

<sup>a</sup> Number of member stars, confirmed by radial velocity, with measured  $[\text{Fe}/\text{H}]$ . This number is less than the total number in SG07 because we exclude spectra with  $\text{S}/\text{N} \lesssim 10 \text{ \AA}^{-1}$ .

<sup>b</sup> We adopt luminosities of Martin et al. (2008) except for LeoT, for which we adopt the luminosity of Irwin et al. (2007).

<sup>c</sup> Average spectral signal-to-noise ratio per  $\text{\AA}$ .

efit from comparing DEIMOS CaT EWs to those of Rutledge et al. for the same globular clusters. Regardless, HIRES observations have confirmed the synthetic metallicities, and we do not consider CaT metallicities any further.

Figure 2 shows three example spectra at three different metallicities. The spectra were chosen to have similar  $T_{\text{eff}}$  and relatively high S/N. Synthetic spectra are also shown, as well as the residuals, which scatter evenly about zero except for a few upward spikes that coincide with incompletely subtracted sky emission lines. These examples demonstrate the ability for neutral iron lines to discriminate easily between stars with different (very low) metallicities even at moderate spectral resolution.

### 3. $[\text{Fe}/\text{H}]$ DISTRIBUTIONS OF THE ULTRA-FAINT DSPHS

For each dSph that SG07 observed, Table 1 shows the number of stars we analyze, mean  $[\text{Fe}/\text{H}]$ , the rms dispersion in  $[\text{Fe}/\text{H}]$ , and the distribution of S/N. The  $[\text{Fe}/\text{H}]$  values are calculated based on weighting by the inverse square of the errors on  $[\text{Fe}/\text{H}]$ . These metallicity measurements establish some of these dSphs as the least enriched known stellar systems, more metal-poor than any GC. In comparison to the CaT metallicities of SG07, the mean metallicities we measure for the dSphs are  $> 0.2$  dex lower for five of the dSphs. Additionally, we find much larger dispersions in  $[\text{Fe}/\text{H}]$  than SG07.

#### 3.1. Metal-poor tail

We present the first case for stars more metal-poor than  $[\text{Fe}/\text{H}] = -3.0$  in dSphs. This data set contains 15 such stars in seven dSphs. Only UMaII contains no stars with  $[\text{Fe}/\text{H}]_{\text{synthetic}} < -3.0$ , although it does contain two stars with  $[\text{Fe}/\text{H}]_{\text{HIRES}} < -3.0$ . To assess the significance of these detections, we compare the metal-poor tail of the MDF for all the ultra-faint dSphs to the Fornax MDF of H06. We choose the conservative metallicity cut of  $[\text{Fe}/\text{H}] < -2.0$ , which includes 178 ultra-faint dSph stars and 83 Fornax stars. For each star in the metal-poor tail of the SG07 sample, we randomly select one counterpart from the metal-poor tail in Fornax with replacement. We then randomly resample the H06  $[\text{Fe}/\text{H}]_{\text{CaT}}$  measurement for the Fornax star from a

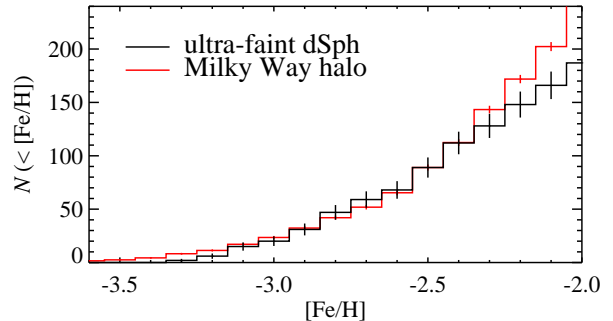


FIG. 3.— Cumulative MDFs for the metal-poor tails of the eight ultra-faint dSphs (black) and the MW halo (red, Beers et al. 2005). The red histogram is normalized to contain the same number of stars with  $[\text{Fe}/\text{H}] < -2.45$  as the black histogram. The error bars are Poissonian.

normal distribution whose standard deviation is given by the uncertainty ( $\delta[\text{Fe}/\text{H}]$ ) for its counterpart in the SG07 sample. At  $[\text{Fe}/\text{H}] < -2.0$ ,  $\delta[\text{Fe}/\text{H}]$  does not vary with metallicity.

After each star in the SG07 sample has been paired in this way, we count the number of stars with  $[\text{Fe}/\text{H}] < -3.0$  in the resampled Fornax distribution. With  $10^6$  Monte-Carlo resampling realizations, the number distribution of stars with  $[\text{Fe}/\text{H}] < -3.0$  appears roughly Poissonian with a median frequency of 5. Just 47 realizations contained 15 stars with  $[\text{Fe}/\text{H}] < -3.0$ . Therefore, we conclude that the probability that our detection of 15 stars with  $[\text{Fe}/\text{H}] < -3.0$  is consistent with being drawn from the H06 Fornax MDF is very low:  $P_{\text{For}} = 4.7 \times 10^{-5}$ . We repeat this test with the other three H06 MDFs to determine  $P_{\text{Scl}} = 3.4 \times 10^{-5}$ ,  $P_{\text{Car}} = 2.5 \times 10^{-5}$ , and  $P_{\text{Sex}} = 4.1 \times 10^{-3}$ . Although Sculptor contains the lowest  $[\text{Fe}/\text{H}]$  measurement in the sample of H06, the Sextans MDF is the most heavily weighted toward low metallicities and therefore has the highest probability of consistency with our sample. These statistical tests are quite conservative and do not consider that we actually detect stars as low as  $[\text{Fe}/\text{H}] = -3.26$ .

In light of the claim by H06 that For, Scl, Car, and Sex lack the metal-poor tail of stars that is present in the MW halo, we compare the newly measured MDFs of the ultra-faint dSphs to the MW halo MDF. Figure 3 shows the metal-poor end of the halo cumulative MDF from the HK and Hamburg/ESO Surveys with carbon-enhanced stars removed (Beers et al. 2005) compared to the cumulative MDF for all eight ultra-faint dSphs combined. The halo histogram is normalized to the number of ultra-faint dSph stars with  $[\text{Fe}/\text{H}] < -2.45$  in order to mute the incompleteness of the halo MDF at higher  $[\text{Fe}/\text{H}]$ . This rough comparison can be done more rigorously when a more complete halo MDF becomes available. In the meantime, the shape of the metal-poor halo MDF looks qualitatively similar to the ultra-faint dSph MDF. Note that the latter MDF covers a narrower dSph luminosity range than the broad spectrum of dSphs which presumably built the stellar halo. As a result, the ultra-faint dSph MDF will cover a narrower metallicity range than the halo MDF.

#### 3.2. Luminosity-metallicity relation

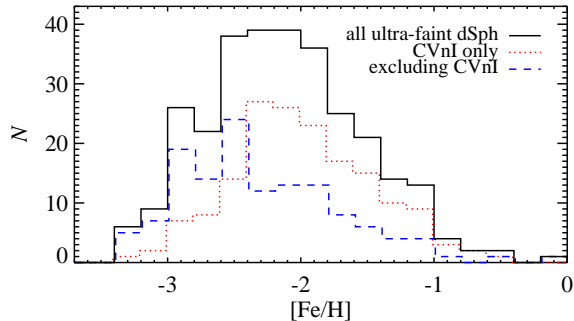


FIG. 4.— Complete MDFs for all eight ultra-faint dSphs (black), for CVnI only (red dotted), and for all ultra-faint dSphs except CVnI (blue dashed). CVnI is the most luminous and metal-rich of those presented here, and it is also the most metal-rich.

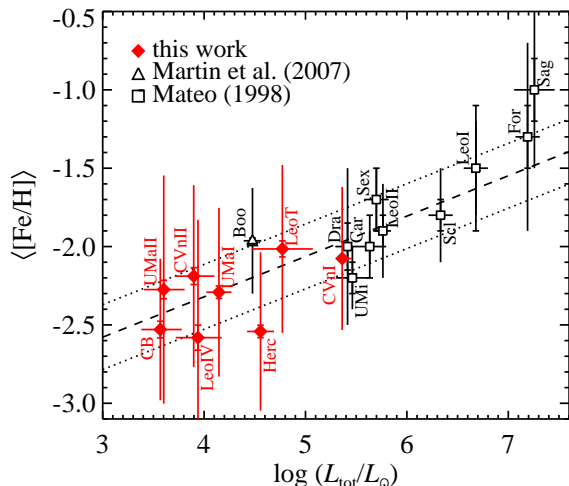


FIG. 5.— The mean  $[\text{Fe}/\text{H}]$  of MW dSphs vs. total luminosity. The dashed line is the weighted, least-squares straight line fit in  $\log(L)$ - $[\text{Fe}/\text{H}]$  space, accounting for the errors in both  $L$  and  $[\text{Fe}/\text{H}]$  (Akritas & Bershadsky 1996). The dotted lines are the rms dispersion of the residuals. The full vertical error bars are the rms dispersions of  $[\text{Fe}/\text{H}]$  within a single galaxy, and the hash marks are the errors on  $\langle [\text{Fe}/\text{H}] \rangle$ . The MW satellite luminosity-metallicity relation is well-defined for 4 dex in luminosity.

Figure 4 shows the complete MDF for all eight dSphs, spanning the range  $-3.3 < [\text{Fe}/\text{H}] < -0.1$ . Because CVnI is significantly more luminous and more metal-rich, we also display its MDF separately.

The segregation by luminosity of the ultra-faint dSph MDFs leads us to redetermine the luminosity-metallicity relation for all MW dSphs except the least luminous objects (Willman 1, Segue 1, and Boötes II). These objects have only a few RGB stars, and their metallicities are not

well known. Figure 5 combines  $[\text{Fe}/\text{H}]$  and  $L$  compiled by Mateo (1998) and Martin et al. (2007) with data for the ultra-faint dSphs (Table 1). The ultra-faint dSphs alone show only weak trends. However, the full 4 dex range of luminosity shows a well-defined relation.

The following equation describes the fit, where the errors are estimates of the standard deviations of the slope and intercept:

$$\langle [\text{Fe}/\text{H}] \rangle = (-2.06 \pm 0.05) + (0.26 \pm 0.07) \log \left( \frac{L_{\text{tot}}}{10^5 L_{\odot}} \right)$$

The linear Pearson correlation coefficient for the data is 0.89, indicating a highly significant correlation.

#### 4. CONCLUSIONS

We have presented metallicity statistics for eight of the least luminous known galaxies in the Universe. We also measure, for the first time, stars outside the MW field halo population with  $[\text{Fe}/\text{H}] < -3.0$ . Furthermore, we have shown that the distribution of  $[\text{Fe}/\text{H}]$  in present-day dSphs reaches nearly as low as that of the MW stellar halo, and that the dSph luminosity-metallicity relation is well-defined for 4 dex in luminosity.

Two differences between our study and previous work have led to our discovery of extremely metal-poor stars in MW dSphs. First, our spectrum synthesis approach is valid for any metallicity and is not restricted to calibrated ranges, like the CaT technique. Second, we explored very faint dSphs whereas H06 examined more luminous dSphs. This work has uncovered very metal-poor stars only in the faintest dSphs, and we do not address their absence or existence in the brighter dSphs.

$[\text{Fe}/\text{H}]$  is just one abundance puzzle in the role of dSphs in building the stellar halo. Most notably,  $[\alpha/\text{Fe}]$  for dSph stars is on average lower than the stars in the halo (e.g., Shetrone et al. 2003; Geisler et al. 2007). However, cosmologically motivated models including star formation and chemical enrichment (Robertson et al. 2005; Font et al. 2006) may explain the difference. These models along with the discovery of very metal-poor stars in surviving dSphs support the original paradigm of galaxy formation (e.g., Searle & Zinn 1978; White & Rees 1978).

We thank Jennifer Johnson, Kim Venn, and the referee for valuable advice. We acknowledge National Science Foundation grants AST-0307966 and AST-0607852 and NASA/STScI grants GO-10265.02 and GO-10134.02. E.N.K. is supported by a NSF Graduate Research Fellowship. A.F. acknowledges support through the W. J. McDonald Fellowship of the McDonald Observatory.

*Facility:* Keck:II (DEIMOS)

#### REFERENCES

- Akritas, M. G., & Bershadsky, M. A. 1996, *ApJ*, 470, 706  
 Battaglia, G., Irwin, M., Tolstoy, E., Hill, V., Helmi, A., Letarte, B., & Jablonka, P. 2008, *MNRAS*, 383, 183  
 Battaglia, G., et al. 2006, *A&A*, 459, 423  
 Beers, T. C., et al. 2005, *From Lithium to Uranium: Elemental Tracers of Early Cosmic Evolution*, 228, 175  
 Bosler, T. L., Smecker-Hane, T. A., & Stetson, P. B. 2007, *MNRAS*, 378, 318  
 Bullock, J. S., & Johnston, K. V. 2005, *ApJ*, 635, 931  
 Choi, P. I., Guhathakurta, P., & Johnston, K. V. 2002, *AJ*, 124, 310  
 Chonis, T. S., & Gaskell, C. M. 2008, *AJ*, 135, 264  
 Font, A. S., Johnston, K. V., Bullock, J. S., & Robertson, B. E. 2006, *ApJ*, 638, 585  
 Geisler, D., Wallerstein, G., Smith, V. V., & Casetti-Dinescu, D. I. 2007, *PASP*, 119, 939  
 Gilbert, K. M., et al. 2007, *ApJ*, 668, 245  
 Guhathakurta, P., et al. 2006, *AJ*, 131, 2497

- Helmi, A., et al. 2006, *ApJ*, 651, L121
- Howley, K. M., Geha, M., Guhathakurta, P., Montgomery, R. M., Laughlin, G., & Johnston, K. V. 2008, *ApJ*, in press (arXiv:0804.0798)
- Ibata, R. A., Gilmore, G., & Irwin, M. J. 1994, *Nature*, 370, 194
- Ibata, Irwin, Ferguson, Lewis & Tanvir, 2001, *Nature*, 412, 49
- Irwin, M. J., et al. 2007, *ApJ*, 656, L13
- Kirby, E. N., Guhathakurta, P., & Sneden, C. 2008, *ApJ*, in press (arXiv:0804.3590)
- Koch, A., Grebel, E. K., Kleyna, J. T., Wilkinson, M. I., Harbeck, D. R., Gilmore, G. F., Wyse, R. F. G., & Evans, N. W. 2007a, *AJ*, 133, 270
- Koch, A., Grebel, E. K., Wyse, R. F. G., Kleyna, J. T., Wilkinson, M. I., Harbeck, D. R., Gilmore, G. F., & Evans, N. W. 2006, *AJ*, 131, 895
- Koch, A., Wilkinson, M. I., Kleyna, J. T., Gilmore, G. F., Grebel, E. K., Mackey, A. D., Evans, N. W., & Wyse, R. F. G. 2007b, *ApJ*, 657, 241
- Martin, N. F., de Jong, J. T. A., & Rix, H.-W. 2008, *ArXiv e-prints*, 805, arXiv:0805.2945
- Martin, N. F., Ibata, R. A., Chapman, S. C., Irwin, M., & Lewis, G. F. 2007, *MNRAS*, 380, 281
- Mateo, M. L. 1998, *ARA&A*, 36, 435
- Robertson, B., Bullock, J. S., Font, A. S., Johnston, K. V., & Hernquist, L. 2005, *ApJ*, 632, 872
- Rutledge, G. A., Hesser, J. E., & Stetson, P. B. 1997, *PASP*, 109, 907
- Searle, L., & Zinn, R. 1978, *ApJ*, 225, 357
- Shetrone, M. D., Côté, P., & Sargent, W. L. W. 2001, *ApJ*, 548, 592
- Shetrone, M., Venn, K. A., Tolstoy, E., Primas, F., Hill, V., & Kaufer, A. 2003, *AJ*, 125, 684
- Simon, J. D., & Geha, M. 2007, *ApJ*, 670, 313
- Tolstoy, E., Irwin, M. J., Cole, A. A., Pasquini, L., Gilmozzi, R., & Gallagher, J. S. 2001, *MNRAS*, 327, 918
- Tolstoy, E., et al. 2003, *AJ*, 125, 707
- Tolstoy, E., et al. 2004, *ApJ*, 617, L119
- White, S. D. M., & Rees, M. J. 1978, *MNRAS*, 183, 341